J Low Temp Phys (2014) 176:712–718
DOI 10.1007/s10909-013-0999-y

In Situ Time Constant and Optical Efficiency Measurements of TRUCE Pixels in the Atacama B-Mode Search

S. M. Simon · J. W. Appel · H. M. Cho · T. Essinger-Hileman · K. D. Irwin · A. Kusaka · M. D. Niemack · M. R. Nolta · L. A. Page · L. P. Parker · S. Raghunathan · J. L. Sievers · S. T. Staggs · K. Visnjic

Received: 15 July 2013 / Accepted: 30 November 2013 / Published online: 18 December 2013

Abstract The Atacama B-mode Search (ABS) instrument, which began observation in February of 2012, is a crossed-Dragone telescope located at an elevation of 5,100 m in the Atacama Desert in Chile. The primary scientific goal of ABS is to measure the B-mode polarization spectrum of the Cosmic Microwave Background from multipole moments of about $\ell \approx 50$ to $\ell \approx 500$ (angular scales from $\sim 0.4°$ to $\sim 4°$), a range that includes the primordial B-mode peak from inflationary gravitational waves. The ABS focal plane array consists of 240 pixels designed for observation at 145 GHz by the TRUCE collaboration. Each pixel has its own individual, single-moded feedhorn and contains two transition-edge

S. M. Simon (✉) · A. Kusaka · L. A. Page · L. P. Parker · J. L. Sievers · S. T. Staggs · K. Visnjic
Department of Physics, Princeton University, Princeton, NJ 08544, USA
e-mail: smstwo@princeton.edu

J. W. Appel · T. Essinger-Hileman
Department of Physics and Astronomy, Johns Hopkins University, Baltimore, MD 21218, USA

H. M. Cho · K. D. Irwin
National Institute of Standards and Technology, Boulder, CO 80305, USA

K. D. Irwin
Department of Physics, Stanford University, Stanford, CA 94305, USA

M. D. Niemack
Department of Physics, Cornell University, Ithaca, NY 14853, USA

M. R. Nolta
The Canadian Institute for Theoretical Astrophysics, University of Toronto,
Toronto, ON M5S 3H8, Canada

S. Raghunathan
Department of Astronomy, Universidad de Chile, Santiago, Chile

sensor bolometers coupled to orthogonal polarizations that are read out using time domain multiplexing. We will report on the current status of ABS and discuss the time constants and optical efficiencies of the TRUCE detectors in the field.

Keywords Atacama B-mode Search · Cosmic Microwave Background · Polarization

1 Introduction

The primary scientific goal of Atacama B-mode Search (ABS) is to measure the polarized signal in the Cosmic Microwave Background (CMB) left by inflationary gravitational waves. Formed at recombination through Thomson scattering, the linear polarization of the CMB can be decomposed into even (E-mode) and odd (B-mode) parity components. Inflationary expansion in the early universe would have produced gravitational waves, which would produce both E-mode and B-mode polarizations at decoupling. However, E-modes can also be formed by scalar density perturbations, making the primordial B-mode signal the clearest evidence for inflation. The primordial B-mode peak is predicted to be on degree angular scales ($l \approx 100$), and its amplitude would give the energy scale of inflation, which varies with different inflationary models [1–3]. While E-modes have been well characterized, primordial B-modes have yet to be measured and are expected to be at least two orders of magnitude below the E-mode spectrum, making their detection an observational challenge [4].

2 The Atacama B-Mode Search Instrument

The ABS instrument is designed to measure the B-mode polarization spectrum of the CMB on large angular scales ($\sim$0.4° to $\sim$4° or $50 \lesssim \ell \lesssim 500$), and has the key characteristics shown in Table 1 [5]. ABS is a cryogenic crossed-Dragone telescope located at an elevation of 5,100 m in the Atacama Desert in Chile, where it can make cross-linked maps. The crossed-Dragone configuration is optimized for low cross-polarization and a clean beam with no need for cryogenic lenses and employs 60 cm mirrors cooled to 4 K by a system of two pulse-tube coolers to reduce loading

Table 1 ABS key characteristics

Parameter	Value	Units
Bolometers	480	
Base temperature	300	mK
Angular resolution	33	Arcminutes (FWHM)
Frequency coverage	127–163	GHz
Sky coverage	$\sim$ 4000	Square degrees
Receiver NEQ[a]	$\sim$30	$\mu K\sqrt{s}$
Detector time constants	$\gtrsim$50	Hz
Polarization modulation	10	Hz
Location	Ground (Chile)	

[a] Noise equivalent sensitivity to a single linear Stokes parameter (Q or U)

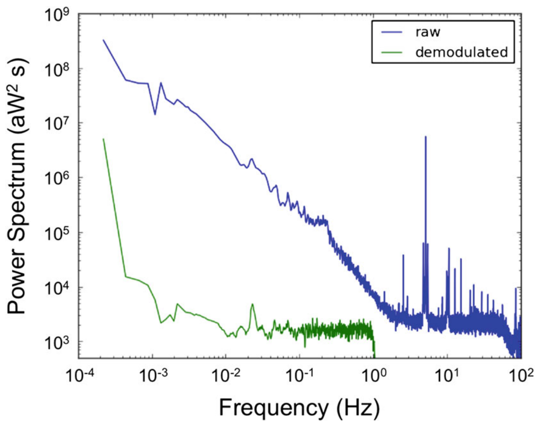

Fig. 1 The decrease in 1/*f* noise from demodulating the HWP signal from a single detector timestream is shown to the right. The raw spectrum has a large low frequency signal with a slow roll-off, while the demodulated spectrum is flat to mHz frequencies. Image courtesy of T. Essinger-Hileman. (Color figure online)

and increase sensitivity. The detectors are read out using time domain multiplexing to limit the number of cryogenic wires and thus reduce the thermal loading on the focal plane, which is cooled to 300 mK by a ^{3}He/^{4}He adsorption refrigerator system [6].

ABS also features a warm half-wave plate (HWP) used for fast, continuous polarization modulation. The HWP is a 330 mm diameter α-cut sapphire plate with a 305 μm anti-reflective coating of Rogers RT/Duroid fluoropolymer laminate that is rotated continuously on air bearings [6]. The HWP rotates at 2.5 Hz, modulating the polarization at 10 Hz and eliminating the need for pair differencing. The ∼1 % emission from the warm HWP leads to only a ∼5 % reduction in sensitivity. The modulation is good for controlling systematics and reduces the sensitivity loss associated with filtering the timestreams. The HWP modulation suppresses 1/*f* noise, which arises primarily from the atmosphere, but also from bath fluctuations and/or readout electronics. Spectra of raw and demodulated data from a single detector timestream of one hour are plotted in Fig. 1. The preliminary median knee frequency of the detectors is ∼1 mHz, and a study is underway to improve knowledge of this value.[1]

Designed for operation at 145 GHz and fabricated at the National Institute of Standards and Technology [5,7], the ABS focal plane array contains 240 TRUCE[2] pixels (Fig. 2) arranged into 24 triangular pods of ten. Each pixel has two transition-edge sensor (TES) bolometers coupled to orthogonal polarizations from a planar ortho-mode transducer (OMT) and an individually machined Al, single-moded corrugated feedhorn coupled to the pixel with a waveguide [8]. The feedhorn angles are optimized to minimize beam mismatch between the two polarizations on each pixel [6]. The signals from the OMT are sent down superconducting Nb through band-defining in-line stub filters. The Nb lines terminate in a lossy Au meander on the silicon nitride membrane comprising the TES island. Each TES is a MoCu bilayer that is kept stable via negative electrothermal feedback.

1 Further details on the HWP performance will be given in an upcoming paper.

2 http://casa.colorado.edu/~henninjw/TRUCE/TRUCE.html.

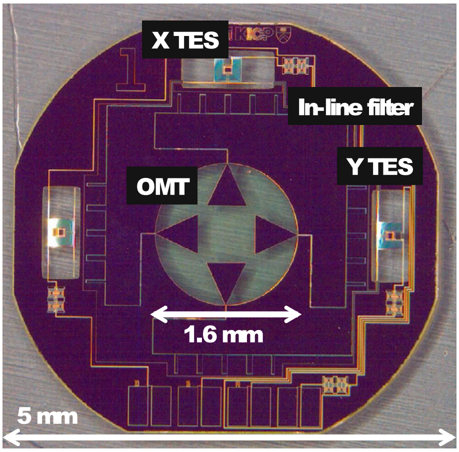

Fig. 2 Each TRUCE pixel has two detectors coupled to orthogonal polarizations. The in-line filters define a band centered around 145 GHz. (Color figure online)

3 Detector and Instrument Characterization

To attain the level of sensitivity necessary to measure the faint B-mode signal, the ABS receiver must be well characterized. The ABS focal plane is made up of four different wafers that were produced in separate fabrications. Because changes in fabrication can impact the detector properties, it is important to characterize the full array. Routine constant azimuth elevation scans (sky dips) and observations of the moon, Saturn, Jupiter, Venus, and RCW 38 are used for calibrating the beam, pointing, and the detector optical efficiencies. Preliminary Fourier Transform Spectrometer (FTS) and time constant data have also been taken for the full array at the site. Additionally, wire grid measurements and observations of Tau A are made periodically to characterize the detector polarization angles and responsivity. We will discuss the time constant and optical efficiency measurements in detail, and other measurements will be described in future publications.

3.1 Time Constants

The time constant of each detector is an important quantity that, if too large, must be accounted for in the demodulation of the signal from the HWP polarization modulation at 10 Hz. The time constants were characterized using the phase delay in the HWP signal modulation instead of the more standard method of using the amplitude of a source with varying modulation frequency. For each phase method measurement, data were taken while slowly varying the rotation speed of the HWP with a sparse polarizing wire grid made of thin (0.005$''$) and reflective Manganin wires on a 1$''$ pitch positioned 4.8$''$ above the HWP. The wire grid, which was perpendicular to the optical axis and covered the entire beam, was used to input a polarized signal of $\sim$0.1 pW. The phase ϕ found from demodulating the signal with respect to the polarization modulation frequency f is the difference between the physical polarization angle of the grid and the measured polarization angle, which includes the apparent angle rotation due to

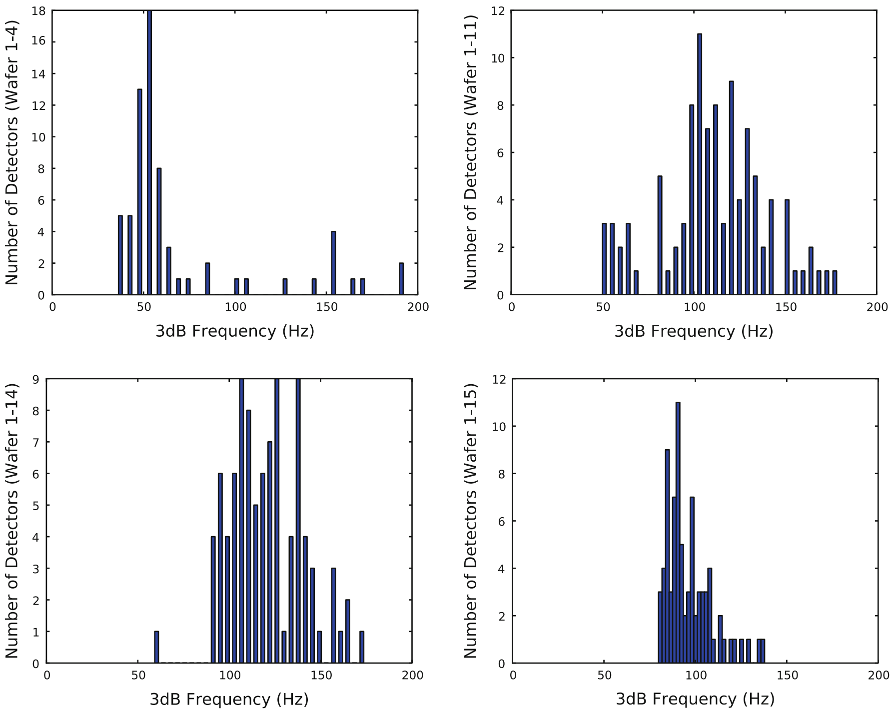

Fig. 3 Above are distributions of 3dB frequencies for the four wafers and for individual detectors in the ABS focal plane. Note that there are 18 detectors with 3dB frequencies above 200 Hz, but the frequency scale has been truncated at 200 Hz for clarity. (Color figure online)

the time delay of the detector response and can be modeled as the phase of a one-pole filter: $\phi = -\arctan(f_{3dB}/f)$, where f_{3dB} is the 3dB frequency of the detector and is inversely related to the time constant τ by $2\pi f_{3dB} = 1/\tau$. Because f^2 is expected to be much less than f_{3dB}^2, the phase can be linearly approximated as $\phi \approx \phi_0 + \frac{f}{f_{3dB}}$, where ϕ_0 is a constant offset related to the intrinsic polarization angle of the detector. Figure 3 shows histograms of the preliminary 3dB frequencies determined by linear fits from a single 20 minute measurement for each wafer. There are 18 detectors with f_{3dB} values greater than 200 Hz that have been excluded from the figures for clarity. The small time constants of these detectors have not been correlated with any effects and they are sufficiently small that they would not need to be corrected for in the timestreams. The median values of the f_{3dB} distributions found from all fit detectors on each wafer are 57^{+101}_{-8} Hz for wafer 1–4, 115^{+40}_{-24} Hz for wafer 1–11, 120^{+21}_{-18} Hz for wafer 1–14, and 92^{+15}_{-7} Hz for wafer 1–15. The upper and lower limits indicate the spread among detectors within each wafer with the boundaries containing 34.1 % of the fit detectors above and below the median. The average percent difference between the f_{3dB} values for each detector between the two sets of measurements is 6 %, consistent with changes expected from atmospheric loading changes (the dominant systematic effect). Even the lowest median f_{3dB} value only causes a 3 % signal reduction, indicating that the detectors are fast enough to respond to the 10 Hz polarization modulation of the HWP.

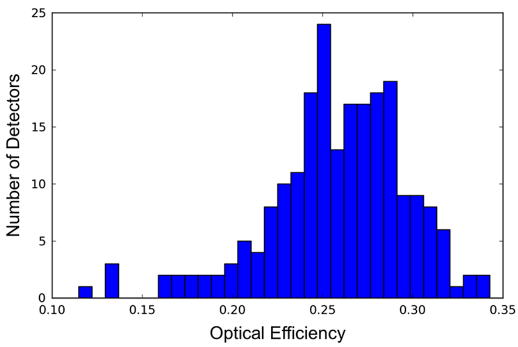

Fig. 4 Preliminary values of the optical efficiency for detectors in the top half of the array are shown to the right [8]. (Color figure online)

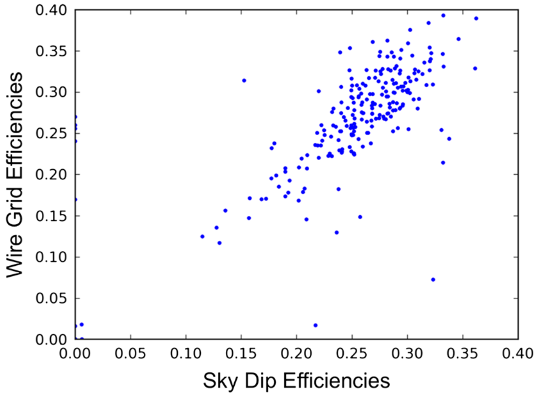

Fig. 5 The sky dip and wire grid methods for determining the optical efficiency are consistent as shown to the right [8]. (Color figure online)

3.2 Optical Efficiency Measurements

One important characteristic is the total optical efficiency of the receiver. The detector response, which depends on the elevation angle, atmospheric conditions, and detector efficiency, is found by measuring the peak-to-peak amplitude from sky dip measurements, which are elevation scans at a constant azimuth position. The dependencies on the elevation angle and the atmospheric conditions can be removed to isolate the relative efficiencies for each detector, and observations of Jupiter with a small number of detectors provide an absolute calibration. Preliminary optical efficiency measurements for the top half of the array are shown in Fig. 4, where the average optical efficiency of the detectors (45 %) and the ∼30 % absorption by the cryogenic stop are the main contributions. Relative efficiencies were also determined by measuring the relative detector responses to a polarized input signal, again produced by placing the sparse wire grid above the instrument. This method is consistent with the sky dip method as shown in Fig. 5. Both analyses assume that the detectors have the same bandpass and beam size and that they observe the same atmospheric signal across the array after the elevation dependence is removed. Analyses of similar measurements from the bottom half of the array are underway as is a full treatment of chromatic effects [8].

4 Summary

ABS was deployed to Chile in February of 2012, and began its second season of observation in March of 2013. ABS observes a large, low-foreground primary field in the Southern Hole and a smaller secondary field with low foregrounds. Maps from the first season of data are in production, and an ABS upgrade is in development. The HWP suppresses $1/f$ noise to $\sim$1 mHz. The detectors are fast enough to allow 10 Hz polarization modulation, and the phase measurement technique allows for good measurement of the time constants. Preliminary calibrations of the ABS detectors have been made, and two different measurement methods are in good agreement on the optical efficiency.

Acknowledgments This work is supported by a NASA Office of the Chief Technologist's Space Technology Research Fellowship. Work at NIST is supported by the NIST Innovations in Measurement Science Program. Work at Princeton University is supported by the NSF through awards PHY-0355328 and PHY-085587, NASA through award NNX08AE03G, and Wilkinson Misrahi funds. Akito Kusaka acknowledges the Dicke Fellowship.

References

1. M. Kamionkowski, A. Kosowsky, A. Stebbins, Phys. Rev. Lett. **78**, 2058 (1997)
2. U. Seljak, M. Zaldarriaga, Phys. Rev. Lett. **78**, 2054 (1997)
3. M. Kamionkowski, A. Kosowsky, A. Stebbins, Phys. Rev. D. **55**, 7368 (1997)
4. D. Baumann et al., AIP Conf. Ser. **1141**, 10 (2009)
5. T. Essinger-Hileman et al., AIP Conf. Ser. **1185**, 494 (2009)
6. T. Essinger-Hileman, *Probing Infationary Cosmology: The Atacama B-Mode Search (ABS)*. Ph.D. Thesis, Princeton University, 2011
7. K.W. Yoon et al., AIP Conf. Ser. **1185**, 515 (2009)
8. K. Visnjic, *Data Characteristics and Preliminary Results from the Atacama B-Mode Search (ABS)*. Ph.D. Thesis, Princeton University, 2013